Available online at www.sciencedirect.com
SCIENCE DIRECT®
Journal of Solid State Chemistry 177 (2004) 889–894
JOURNAL OF SOLID STATE CHEMISTRY
http://elsevier.com/locate/jssc

Structure of β-$AgAlO_2$ and structural systematics of tetrahedral $MM'X_2$ compounds

J. Li and A.W. Sleight*

Department of Chemistry, Oregon State University, Gilbert 153, Corvallis, OR 97331-4003, USA

Received 17 July 2003; received in revised form 16 September 2003; accepted 24 September 2003

Abstract

The structure of β-$AgAlO_2$ has been refined from neutron diffraction data by the Rietveld method. The space group is $Pna2_1$ with $a = 5.4306(1)$ Å, $b = 6.9802(1)$ Å, $c = 5.3751(1)$ Å, and $Z = 4$. Both cations are tetrahedrally coordinated to oxygen. The tetrahedron around Al is quite regular with distances ranging from 1.75 to 1.77 Å and angles ranging from 107.8 to 111.0°. The tetrahedron around Ag is, however, highly distorted with distances ranging from 2.35 to 2.48 Å and angles ranging from 99.3 to 131.6°. The low bond valence calculated for Ag(I) of 0.895 is attributed to the strong deviation of the O–Ag–O angles from 109.5°. This structure is based on the hexagonal ZnO structure, and we show that the ordered arrangement of M(I) and M(III) cations in this structure directly causes the tetrahedra to distort and tilt.

Keywords: Neutron diffraction; Crystal Structure; Tetrahedral compounds; $AgAlO_2$; Silver aluminum oxide

1. Introduction

Two forms of $AgAlO_2$ have been reported [1–3]. Reaction of $LiAlO_2$ with molten $AgNO_3$ gives α-$AgAlO_2$, which has the delafossite structure where Al is octahedrally coordinated and Ag is in two-fold linear coordination to oxygen [1]. This form has also been prepared at high pressure by a direct reaction between Ag_2O and Al_2O_3 [2]. Crystals obtained in this reaction were used for a refinement of the structure [2]. Reaction of β-$NaAlO_2$ with molten $AgNO_3$ or an aqueous solution of $AgNO_3$ gives β-$AgAlO_2$ [3]. Based on a comparison of X-ray powder diffraction patterns, it was concluded that β-$AgAlO_2$ is isomorphous with β-$NaAlO_2$, a structure in which all atoms are tetrahedrally coordinated. We present here for the first time a refinement of the orthorhombic β-$AgAlO_2$ structure, which is based on the hexagonal ZnO structure. It has been reported that both $AgFeO_2$ and $AgGaO_2$ can also be prepared in this structure; however, neither positional parameters nor cell edges were given [4,5].

The structures of hexagonal ZnO and cubic ZnS may be viewed as tetrahedra sharing corners. Replacing divalent Zn with equal amounts of univalent and trivalent cations leads to an extensive series of $MM'X_2$ compounds, known as 136_2 tetrahedral compounds. Nitride and phosphide $MM'X_2$ compounds form an isostructural series of 245_2 compounds with divalent and tetravalent cations. Starting with the cubic structure, ordering of the M and M' cations leads to a tetragonal structure whereas starting with the polar hexagonal structure leads to a polar orthorhombic structure. We discuss the distortions to this orthorhombic $MM'X_2$ structure that necessarily occur when M and M' differ in size.

2. Experimental

$NaAlO_2$ was first prepared by reaction of Al_2O_3 (Aldrich, 99.8%) with a stoichiometric amount of Na_2CO_3 (Aldrich, 99.95–100.05%) at 1050°C for 12 h. This white β-$NaAlO_2$ powder was mixed with $AgNO_3$ (Spectrum, 99.0%) and KNO_3 (Mallinckrodt, 99.97%) using a molar ratio of 1:1.03:1 in an agate mortar. This mixture was pressed into a pellet and heated in air at

*Corresponding author. Fax: +1-541-737-2062.
E-mail addresses: liju@chem.orst.edu (J. Li), arthur.sleight@orst.edu (A.W. Sleight).

0022-4596/$ - see front matter © 2003 Elsevier Inc. All rights reserved.
doi:10.1016/j.jssc.2003.09.036

210°C for 24 h. The resulting pellet was pulverized, washed with water, and dried at room temperature in air. An X-ray diffraction pattern of this product indicates a pure phase of β-$AgAlO_2$ according to ICSD [6].

Neutron powder diffraction data were collected using the BT-1 32-counter high-resolution diffractometer at the NIST Center for Neutron Research at the National Institute of Standards and Technology. A Cu (311) monochromator, yielding a wavelength of 1.5402 Å, was employed. Collimation of 15′, 20′, and 7′ of arc were used before the monochromator, before the sample, and before the detectors, respectively. The sample was loaded in a vanadium can sample container of length 50 mm and diameter 12.4 mm. Data were collected at room temperature over a 2θ range of 3–168°. Rietveld refinement of the neutron data shows an impurity phase of 1.7% α-Al_2O_3.

The β-$AgAlO_2$ structure was also refined using distance least squares (DLS) [7]. In this least-squares refinement, prescribed distances for the bonds and the edges of the tetrahedra are used as the observations.

3. Structure of β-$AgAlO_2$

A Rietveld refinement of the neutron data in space group $Pna2_1$ using GSAS software [8] starting with the positional parameters reported for β-$NaAlO_2$ led to $R_{wp} = 5.71\%, R_p = 4.69\%$, and $\chi^2 = 1.065$ with $a = 5.4306(1)$ Å, $b = 6.9802(1)$ Å, $c = 5.3751(1)$ Å. The cell parameters are very close to those given in PDF file #21-1070I [6]. The final positional and displacement parameters are given in Table 1. One z parameter must be fixed in this structure; thus, z(Al) was fixed at 0.0. Fig. 1 shows the agreement between the observed and calculated neutron diffraction patterns. Interatomic distances and angles are given in Table 2. Fig. 2 shows a fragment of the structure where atoms are given as thermal ellipsoids, and Fig. 3 shows the β-$AgAlO_2$ structure as corner-sharing tetrahedra.

Table 1
Structure refinement results of $AgAlO_2$

	Ag	Al	O1	O2
x	0.0532(4)	0.0610(5)	0.0311(3)	0.1283(3)
y	0.6268(4)	0.1250(6)	0.0723(3)	0.6765(3)
z	0.9968(7)	0.000000	0.3208(8)	0.4344(7)
U_{iso}[a]	1.40(5)	0.59(6)	0.87(4)	0.80(4)
U_{11}	1.73(9)	0.8(2)	1.12(9)	0.78(8)
U_{22}	1.18(8)	0.6(1)	1.04(8)	0.61(8)
U_{33}	1.40(9)	0.7(1)	0.64(7)	1.05(8)
U_{12}	−0.23(8)	−0.3(1)	−0.06(9)	−0.21(7)
U_{13}	−0.23(9)	−0.1(1)	−0.08(9)	−0.05(8)
U_{23}	−0.14(7)	0.1(1)	0.02(8)	0.05(7)
BV[b]	0.895	2.729	1.797	1.827

[a] Thermal displacement parameters (Å^2) are multiplied by 100 and defined as $T = \exp[-2\pi^2(U_{11}h^2a^{*2} + U_{22}k^2b^{*2} + U_{33}l^2c^{*2} + 2U_{12}hka^*b^* + 2U_{13}hla^*c^* + 2U_{23}klb^*c^*)]$.

[b] Bond valences are calculated by VaList [9].

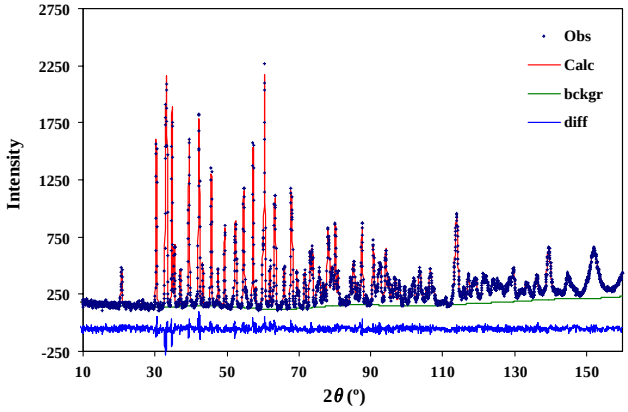

Fig. 1. Observed and calculated neutron diffraction patterns of β-$AgAlO_2$ with the difference pattern below.

Table 2
Bond lengths (Å) and angles (deg)

Ag–O1	2.477(2)	Al–O1	1.771(4)
Ag–O1′	2.349(3)	Al–O1′	1.753(4)
Ag–O2	2.412(3)	Al–O2	1.761(3)
Ag–O2′	2.359(3)	Al–O2′	1.761(4)
O1–Ag–O1′	99.3(1)	O1–Al–O1′	110.2(2)
O1–Ag–O2	103.91(9)	O1–Al–O2	109.0(2)
O1–Ag–O2′	100.9(1)	O1–Al–O2′	107.8(2)
O1′–Ag–O2	107.3(1)	O1′–Al–O2	108.9(2)
O1′–Ag–O2′	131.59(9)	O1′–Al–O2′	110.0(2)
O2–Ag–O2′	109.8(1)	O2–Al–O2′	111.0(2)

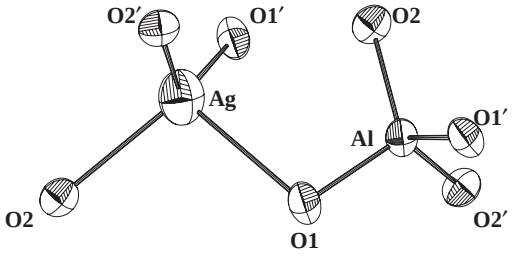

Fig. 2. Structure of β-$AgAlO_2$ using ellipsoids to show relative thermal displacements where anion labels relate to Table 2.

4. Discussion

In a simple cubic lattice each atom has 6 nearest neighbors. A one-to-one ordering of unlike atoms in this lattice can lead to a structure where each atom has only the other atoms as near neighbors, i.e., the NaCl structure. The analogy for one-to-one ordering of

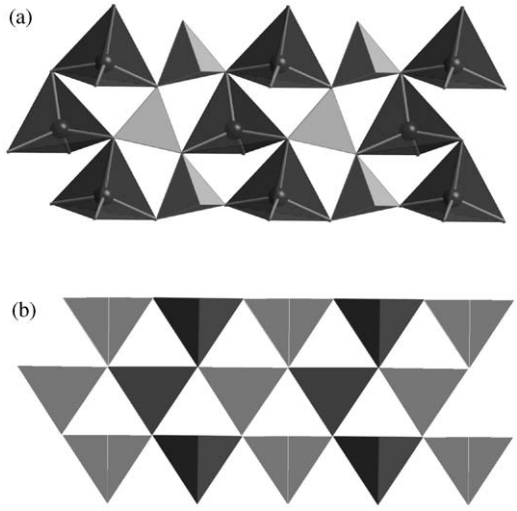

Fig. 3. Structure of β-$AgAlO_2$ as corner-sharing tetrahedral: (a) dark AgO_4 and light AlO_4 tetrahedra, (b) dark and light OAg_2Al_2 tetrahedra with a central O1 and O2 atom, respectively. Same projection for (a) and (b) with the c-axis vertical.

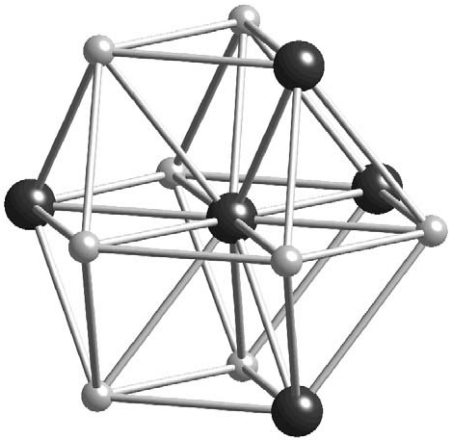

Fig. 4. Near cation environment around Ag where the 8 Ag–Al distances from central Ag range from 3.20 to 3.50 Å and average 3.34 Å, and the 4 Ag–Ag distances range from 3.21 to 3.27 Å and average 3.24 Å. The c-axis is vertical.

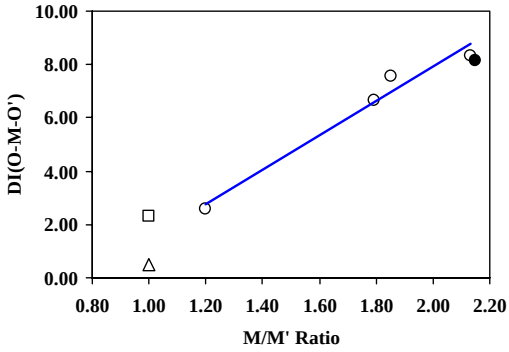

Fig. 5. Angle distortion indexes for the M cation vs. the M/M' radius ratio [10] in orthorhombic $MM'O_2$ compounds. The square and triangle are for hexagonal ZnO [11] and BeO [12], respectively; open circles, from left to right, are for orthorhombic $LiGaO_2$ [13], $NaFeO_2$ [14], $NaGaO_2$ [15] and $NaAlO_2$ [16], respectively; and the solid circle is for $AgAlO_2$ (this work).

cations is found in the AMX_3 perovskite structure where the M cations form a simple cubic lattice. Ordering of M and M' cations leads to the $A_2MM'X_6$ ordered perovskite structure where the M and M' cations have adopted a NaCl type arrangement, and the cubic symmetry can be retained. One-to-one ordering of cations becomes much more complicated starting with either a hexagonal or cubic-closed packed lattice. It is now geometrically impossible to order such that each cation will have only unlike cations as its 12 near neighbors. The most that can be accomplished is to have 8 unlike and 4 like near neighbors. Such ordering leads to a lower symmetry crystal class. Ordering in the cubic ZnS structure leads to tetragonal $MM'X_2$ compounds with a doubling of the unit cell volume. Ordering in the hexagonal ZnO structure leads to orthorhombic $MM'X_2$ compounds with a unit cell volume four times that of ZnO. Fig. 4 shows the cation environment around Ag in β-$AgAlO_2$, which is analogous to the cation environment around Al. This figure shows how the ordering of cations has destroyed the hexagonal symmetry.

The number of variable parameters in the tetragonal tetrahedral $MM'X_2$ structure is three: a, c, and an x parameter for the anion. With just these three parameters, this structure can accommodate M and M' cations of different sizes while maintaining rather regular tetrahedra. The $M-X$ distances are all equal to one another; the $M'-X$ distances are all equal to one another; the angles are all close to the ideal tetrahedral value. The situation is very different for the orthorhombic $MM'X_2$ structure based on the hexagonal ZnO structure. The number of variable parameters is now fourteen: a, b, c, and 11 positional parameters associated with the two cations and the two crystallographically distinct anions. Despite the much greater number of variable parameters in this structure, this structure cannot as easily accommodate M and M' cations of different sizes. Our DLS calculations confirm that undistorted tetrahedra of different sizes cannot link together in this structure. A considerable range of $M-X$ and $M-X'$ bond lengths necessarily develops as the M/M' radius ratio deviates from unity, and the angles deviate strongly from the ideal tetrahedral value. This trend is most pronounced for the angles of the M(I) cation, and angle distortion indexes for the $M(I)$ cation are shown in Fig. 5 for the $MM'O_2$ series. This distortion index is defined as the mean of the absolute value of the difference between the observed angles and the ideal tetrahedral angle of 109.5°. These values can be significant even when the size of M and M' are the same. For example, the angle distortion indexes for BeO and

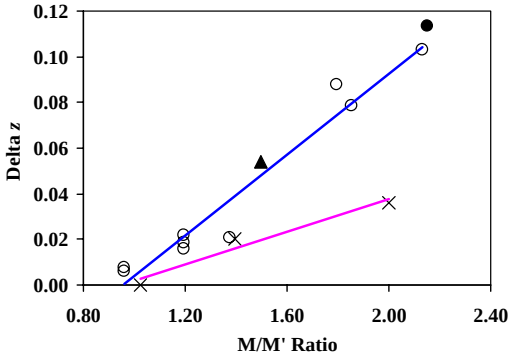

Fig. 6. Anion delta z vs. the M/M' radius ratio in orthorhombic $MM'X_2$ compounds. Open circles, from top to bottom and left to right, are for 136_2 type $MM'X$ compounds $LiInSe_2$ [17], $LiInS_2$ [18], $LiGaO_2$ [13], $LiGaS_2$ [19], $LiGaSe_2$ [19], $LiAlSe_2$ [20], NaFeO2 [14], $NaGaO_2$ [15] and $NaAlO_2$ [16], respectively; solid triangle is for $AgInS_2$ [21] and solid circle is for $AgAlO_2$ (this work); cross points, from left to right, are for 245_2 type $MM'X$ compounds $BeSiN_2$ [22], $ZnGeN_2$ [23] and $MnSiN_2$ [24].

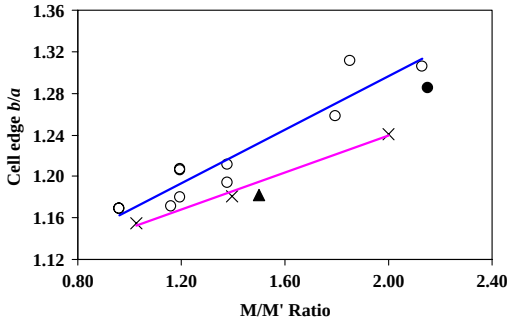

Fig. 7. Cell edge b/a ratio vs. the M/M' radius ratio in orthorhombic $MM'X_2$ compounds. Open circles, from top to bottom and left to right, are for 136_2 type $MM'X$ compounds $LiInSe_2$ [17], $LiInS_2$ [18] (overlapping with $LiInSe_2$), $LiFeO_2$ [25], $LiGaS_2$ [19], $LiGaSe_2$ [19] (overlapping with $LiGaS_2$), $LiGaO_2$ [13], $LiAlSe_2$ [20], $LiAlO_2$ [26], $NaFeO_2$ [14], $NaGaO_2$ [15] and $NaAlO_2$ [16] respectively; solid triangle is for $AgInS_2$ and solid circle is for $AgAlO_2$ [this work]; cross points, from left to right, are for 245_2 type $MM'X$ compounds $BeSiN_2$ [22], $ZnGeN_2$ [23], and $MnSiN_2$ [24].

ZnO are 0.49 and 2.31, respectively. However, these indexes become much larger as the M/M' ratio deviates from unity (Fig. 5).

In the $MM'X_2$ series the cation tetrahedra tilt increasingly as the M/M' ratio deviates from unity. This tilting is shown for β-$AgAlO_2$ in Fig. 3(a). This tilting is indicated by the difference in the z values for the two crystallographically distinct anions in this structure (Fig. 6). These two z values are exactly the same in the hexagonal ZnO structure. The z values for the two cations would also be equal in the hexagonal ZnO structure, and these values remain very nearly the same in the orthorhombic structure. Thus, the anion tetrahedra do not show significant tilting (Fig. 3(b)). Another change that occurs as the M/M' radius ratio deviates from unity is an increase of the b/a ratio (Fig. 7) from its ideal value of 1.155. Our DLS calculations show that both the increase in the b/a ratio and the increase in anion delta z are a direct result of having M and M' cations of different sizes.

Bond valence calculations indicate significant underbonding of Ag in β-$AgAlO_2$ (Table 1). In fact, this is one more trend that correlates with the M/M' radius ratio (Fig. 8). Both M and M' cations appear to become underbonded as the M/M' radius ratio deviates from unity. This is most likely due to a failure of the usual bond valence approach to consider the effect of $X-M-X$ angles or anion–anion repulsion. A $M-X$ distance will be impacted both by the forces between M and X and the forces between X and X, which are not considered. As a regular octahedron distorts, for example to a trigonal prism, anion–anion repulsion increases and the $M-X$ distances are expected to increase. As the anion environment around a cation "distorts" from tetrahedral to square planar, the

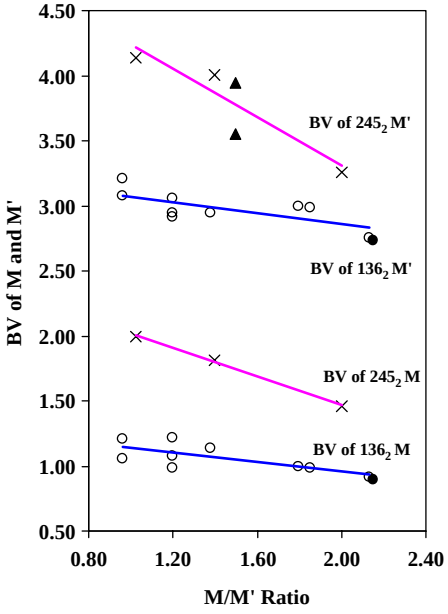

Fig. 8. Bond valences of M and M' vs. the M/M' radius ratio in orthorhombic $MM'X_2$ compounds. Open circles, from top to bottom and left to right, are for 136_2 type $MM'X_2$ compounds $LiInSe_2$ [17], $LiInS_2$ [18], $LiGaSe_2$ [19], $LiGaS_2$ [19], $LiGaO_2$ [13], $LiAlSe_2$ [20], $NaFeO_2$ [14], $NaGaO_2$ [15], $NaAlO_2$ [16]; solid triangles are for $AgInS_2$ [21] (top: BV of Ag, bottom: BV of In) and solid circles are for $AgAlO_2$ (this work); cross points, from left to right, are for 245_2 type $MM'X_2$ compounds $BeSiN_2$ [22], $ZnGeN_2$ [23], and $MnSiN_2$ [24].

increased repulsion between anions is expected to give increased $M-X$ distances. Thus, Shannon [10] gives the radius for tetrahedral Ag(I) to be 1.14 Å and the radius for square planar Ag(I) to be 1.16 Å. Our observed Ag–O distances (Table 2) indicate underbonding only on the assumption of tetrahedral

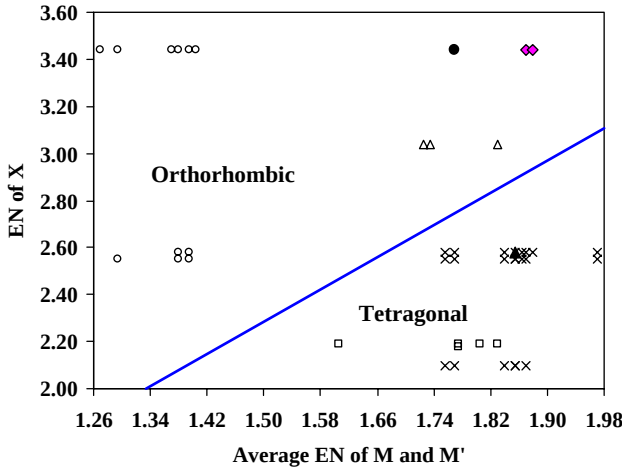

Fig. 9. Stability field for tetragonal vs. orthorhombic $MM'X_2$ compounds. Pauling's electronegativity data were used [28]. Open circles and triangles are for 136_2 and 245_2 type orthorhombic $MM'X_2$ compounds mentioned above in this paper; solid circle is for $AgAlO_2$ [this work] and solid triangle is for $AgInS_2$ [21]; gray diamonds are for $AgFeO_2$ and $AgGaO_2$ [4,5]; cross points and squares are for 136_2 [27] and 245_2 [29] type tetragonal $MM'X_2$ compounds, respectively.

coordination. Although the bond distance approach accounts for the variation of Ag–O bond length, it does not account for the variation in O–Ag–O angles. Our observed distances agree well with Shannon radii if square planar Ag(I) is assumed instead of tetrahedral Ag(I). This may be considered as the appropriate correction when O–Ag–O angles deviate strongly from 109.5°.

It has previously been noted for tetrahedral MX compounds that higher ionicity favors the hexagonal structure over the cubic structure [27]. This is presumably due to the more favorable Madelung constant for the hexagonal structure. Fig. 9 shows the stability field for tetrahedral tetragonal and orthorhombic compounds. Again, it is clear that the orthorhombic structure, which is based on the hexagonal structure, is favored by higher ionicity. Thus, all oxides and nitrides (top two rows) have the orthorhombic structure, and all tellurides and phosphides (bottom two rows) have the tetragonal structure. Both the tetragonal and orthorhombic structures are found for sulfides and selenides (middle two rows), but there is a clear dependency on ionicity. One compound, $AgInS_2$, is known in both structures [21,30]. With only this one exception, the orthorhombic structure is always found when the difference between the electronegativity on the anion and the average value for the cations is greater than 1.1, and the tetragonal structure is always found when this difference is less than 0.9.

Better characterization of orthorhombic $AgInS_2$ might resolve the issue of why it does not lie closer to the tetragonal-orthorhombic border in Fig. 9. The most recent structure study was based on X-ray powder diffraction data on a three-phase sample containing only 23% orthorhombic $AgInS_2$ [21]. All occupation factors were fixed at 100%, and individual thermal displacement factors were not refined. The cations Ag and In cannot be distinguished by X-ray diffraction due to their very similar scattering powers. Apparently no z parameter was fixed, which would likely lead to an unstable refinement. Note that even the b/a parameter for $AgInS_2$ does not fit the trend in Fig. 7. Furthermore, bond valences calculated for Ag and In based on the reported structure [21] are both too big (Fig. 8). Clearly, the structure and composition of "$AgInS_2$" need to be examined more closely.

Acknowledgments

This research was supported by NSF. We thank the NIST Center for Neutron Research at the National Institute of Standards and Technology, US Department of Commerce, for providing the neutron research facilities and University of Maryland Outreach Program for partial support of this work. We are grateful to Dr. B.H. Toby for assistance with collection of the neutron diffraction data.

References

[1] W. Gessner, Z. Anorg. Allg. Chem. 352 (1967) 145.
[2] G. Brachtel, M. Jansen, Cryst. Struct. Commun. 10 (1981) 173.
[3] E. Thilo, W. Gessner, Z. Anorg. Allg. Chem. 345 (1966) 151.
[4] G. Hakvoort, Therm. Anal. Proc. Int. Conf. 4th 1 (1975) 469.
[5] G.A. Korteweg, J. Magn. Reson. 42 (1981) 181.
[6] G. Hakvoort, ICSD 21-1070I $AgAlO_2$, Delft, Netherlands, 1968.
[7] W.M. Meier, H. Villiger, Z. Kristallogr. 129 (1966) 161.
[8] B.H. Toby, J. Appl. Cryst. 34 (2001) 210.
[9] A.S. Wills, I.D. Brown, VaList, CEA, France, 1999, Program available from ftp://ftp.ill.fr/pub/dif/valist/
[10] R.D. Shannon, Acta Crystallogr. A 32 (1976) 751.
[11] O. Garcia-Martinez, R.M. Rojas, E. Vila, J.L. Vidales, Solid State Ionics 63 (1993) 442.
[12] G. Vidal-Valat, J.P. Vidal, K. Kurki-Suonio, R. Kurki-Suonio, Acta Crystallogr. A 43 (1987) 540.
[13] M. Marezio, Acta Crystallogr. 18 (1965) 481.
[14] E.F. Bertaut, A. Delapalme, G. Bassi, J. Phys. (Paris) JOPQA 25 (1964) 545.
[15] H.-P. Muller, R. Hoppe, Z. Anorg. Allg. Chem. 611 (1992) 73.
[16] J.A. Kaduk, S.Y. Pei, J. Solid State Chem. 115 (1995) 126.
[17] W. Hönle, G. Kühn, H. Neumann, Z. Anorg. Allg. Chem. 543 (1986) 161.
[18] Z.Z. Kish, A.S. Kanishcheva, Yu.N. Mikhailov, V.B. Lazarev, E.E. Semrad, E.Yu. Peresh, Dokl. Akad. Nauk SSSR 280 (2) (1985) 398.
[19] L. Isaenko, A. Yelisseyev, S. Lobanov, A. Titov, V. Petrov, J.-J. Zondy, P. Krinitsin, A. Merkulov, V. Vedenyapin, J. Smirnova, Cryst. Res. Technol. 38 (3–5) (2003) 379.
[20] J.Y. Kim, T. Hughbanks, Inorg. Chem. 39 (14) (2000) 3092.
[21] G. Delgado, A.J. Mora, C. Pineda, T. Tinoco, Mater. Res. Bull. 36 (2001) 2507.

[22] P. Eckerlin, Z. Anorg. Allg. Chem. 353 (1967) 225.
[23] M. Wintenberger, M. Maunaye, Y. Laurent, Mater. Res. Bull. 8 (9) (1973) 1049.
[24] M. Maunaye, R. Marchand, J. Guyader, Y. Laurent, J. Lang, Bull. Soc. Fr. Miner. Crystallogr. 94 (5–6) (1972) 561.
[25] Honma Takahiko, Noritake Tatsuo, Ukyou Yoshio, JP 10241688 A2 19980911 Heisei, 1998, 10pp (patent written in Japanese).
[26] K. Dörhöfer, J. Appl. Cryst. 12 (2) (1979) 240.
[27] E. Parthe, Crystal Chemistry of Tetrahedral Structures, Gordon and Breach Science Publishers, New York, 1964, p. 129.
[28] A.L. Allred, J. Inorg. Nucl. Chem. 17 (1961) 215.
[29] J.E. Jaffe, A. Zunger, Phys. Rev. B: Condens. Matter Mater. Phys. 30 (2) (1984) 741.
[30] R.S. Roth, H.S. Parker, W.S. Brower, Mater. Res. Bull. 8 (1973) 333.